Global Journal of Engineering and Technology [GJET].
ISSN: 2583-3359 (Online)
Frequency: Monthly
Published By GSAR Publishers
Journal Homepage Link- https://gsarpublishers.com/journal-gjet-home/

Velocity structure of the Earth's crust and structural control of seismicity in the Krupnik area, Southwestern Bulgaria

By

Emil Oynakov[1] Boyko Ranguelov[2] Irena Aleksandrova[1] Mariya Popova[1]

[1]National Institute of Geophysics, Geodesy and Geography - Bulgarian Academy of Sciences, Acad. G. Bonchev St., bl. 3, 1113 Sofia, Bulgaria

[2] Space Research and Technology Institute - Bulgarian Academy of Sciences, Acad. G. Bonchev St., bl. 1, 1113 Sofia, Bulgaria

Article History

Received: 17/07/2026
Accepted: 25/07/2026
Published: 28/07/2026

Vol – 5 Issue – 7

PP: - 36-43

Abstract

The present study investigates the depth-dependent structure and seismotectonic behavior of the fault zone associated with the 1904 doublet earthquakes in southwestern Bulgaria (4th April, 1904, M7.2 and M7.8 in a time domain of 20 min.). The principal contribution of this study is an integrated interpretation combining previously published local earthquake tomography with updated seismicity, active fault geometry, historical earthquake information, and gravity observations. Despite the availability of geological, geodetic, and geophysical data, the geometry and mechanical behavior of the fault system at depth remain insufficiently constrained.

The results reveal depth-dependent variations in crustal structure. In the 10–15 km depth interval, a comparatively coherent upper–middle crust is inferred from neutral-to-positive Vp and Vs anomalies and strong lateral contrasts in Vp/Vs. This interval is broadly compatible with previous macroseismic depth estimates for the 1904 earthquakes, although the historical focal depths remain uncertain. At depths of 20–30 km, reduced S-wave velocities and elevated Vp/Vs values are observed in parts of the model. These patterns are interpreted cautiously as possible indicators of reduced shear rigidity within the middle crust, potentially related to temperature, fluids, mineralogical variations, or lithological contrasts.

The Krupnik fault is expressed in the analyzed datasets primarily as a structural boundary between crustal domains rather than as a simple localized low-velocity zone; this interpretation is supported qualitatively by the spatial correspondence between tomographic contrasts and Bouguer gravity gradients. Contemporary seismicity exhibits clear structural control by the fault-system geometry, with hypocenters preferentially associated with fault segments and lateral velocity gradients rather than with isolated velocity extremes.

The obtained results support a model of a structurally controlled fault system that might extends into the middle crust, where contemporary seismicity reflects distributed deformation within the investigated fault zone and its immediate crustal surroundings.

Keywords: *Krupnik Fault; seismotectonics; local seismic tomography (Vp, Vs, Vp/Vs), structural control, seismicity.*

Introduction

The Krupnik fault zone in southwestern Bulgaria represents one of the major active tectonic structures within the northern Aegean extensional domain. The region is well documented historically due to the two catastrophic earthquakes of 04 April 1904 (Christoskov L., et al., 1978) with magnitudes of Mw = 6.9 and Mw = 7.2 (Ambraseys, N., 2001). The instrumental observations reveal elevated and spatially concentrated seismicity aligned with active fault segments. Previous macroseismic studies suggest focal depths of approximately 15–18 km for the 1904 earthquakes and magnitudes 7.2 and 7.8, although these estimations remain uncertain due to the absence of instrumental observations (Ranguelov, B., et al., 2001).

*Corresponding Author: Emil Oynakov

Regional tectonic studies indicate that the area is characterized predominantly by extensional to oblique-extensional deformation associated with the active north Aegean tectonic regime (Meyer, B. et al., 2002; Protopopova, V. and E. Botev, 2020). Available focal mechanism solutions indicate predominantly normal faulting, consistent with the present-day regional stress field. The 1904 earthquake sequence is commonly interpreted as one of the strongest continental earthquake doublets in southeastern Europe.

Previous geological, geodetic, and gravimetric studies, including long-term GNSS observations and detailed structural analyses (e.g., Dimitrov, D., et al., 2010), documented block-type deformation and well-defined structural boundaries within the Struma River valley. Despite this extensive dataset, the deep geometry of the active fault system and its mechanical behavior within the middle crust remain insufficiently constrained.

In this study, we apply an integrated approach combining local seismic travel-time tomography (Vp, Vs, and Vp/Vs), instrumental seismicity for the period 1991–2025, mapped surface active faults, and regional gravity data to investigate the depth-dependent structure and deformation of the Simitli–Krupnik fault system. Particular emphasis is placed on the 20–30 km depth interval, where the combined distribution of seismicity, Vs anomalies, and Vp/Vs variations may provide information on changes in middle-crustal properties. Transitions from a brittle, seismogenic upper crust to mechanically weaker middle-crustal conditions at depths of ~20–30 km are widely documented in continental settings (Scholz, C. H., 2002; Bürgmann, R. and Dresen, G., 2008), but their expression beneath the Krupnik fault zone remains poorly constrained.

The novelty of this study lies not in presenting a new tomographic inversion, but in developing an integrated seismotectonic interpretation of the Krupnik fault system by combining previously published local seismic tomography with updated instrumental seismicity, active fault geometry, focal-mechanism information, historical earthquake constraints, and regional gravity observations. Because Vp/Vs anomalies are inherently non-unique, the interpretation emphasizes the spatial complex relationships among velocity structure, seismicity, active faults, and gravity gradients rather than relying on isolated anomaly patterns alone.

Data

The earthquake catalog used in this study covers the period 1991–2025, corresponding to the interval with the most stable digital instrumental coverage for the investigated region. The final dataset includes approximately 12,400 earthquakes after applying spatial and depth-selection criteria. The events were extracted from the Bulgaria Digital Seismic Network – doi.org/10.7914/SN/BS, and hypocentral parameters correspond to routine catalog solutions. Magnitudes are reported as catalog magnitudes. Because focal-depth uncertainty increases with depth and varies with network geometry, deeper hypocentral solutions should be interpreted cautiously, particularly below ~20 km.

Three-dimensional seismic velocity models (Vp and Vs) were adopted from previously published local earthquake tomography developed for the broader Kresna–Krupnik region. Relative velocity anomalies (ΔVp and ΔVs) together with Vp/Vs ratios were analyzed at depth levels of 5, 10, 15, 20, 25, and 30 km using a common one-dimensional reference velocity model.

Active fault traces were compiled primarily from the European Fault-Source Model 2020 (EFSM20), supplemented by published neotectonic maps and regional structural studies related to the 1904 earthquake sequence.

Regional Bouguer gravity anomaly data are reduced using a standard density of 2.67 g/cm³ and provided by Prof. D. Dimitrov (Dimitrov, D., 2019). They were incorporated qualitatively to evaluate large-scale crustal density contrasts and possible structural boundaries associated with the Krupnik fault system.

Instrumental seismicity is spatially concentrated along the Simitli–Krupnik fault zone and adjacent active structures, forming a pronounced WNW–ESE-oriented seismic belt visible both in map view and vertical cross-sections.

Because the present study relies partly on previously published tomographic models and routine earthquake catalog solutions, the interpretation focuses primarily on robust spatial relationships among seismicity, fault geometry, and velocity gradients rather than on individual anomaly amplitudes alone.

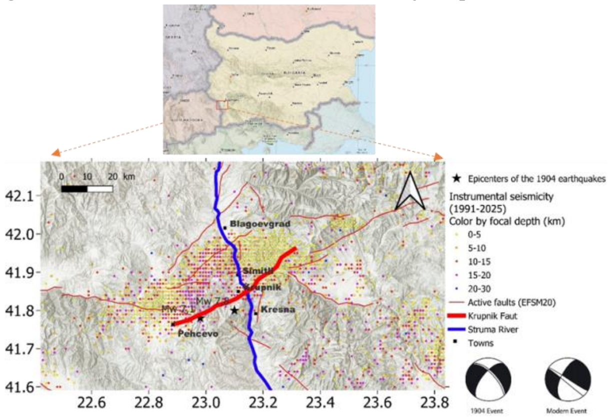

Fig. 1. Regional tectonic framework (a). Contemporary seismicity of the Krupnik fault zone, southwestern Bulgaria. Instrumental seismicity for the period 1991–2025 is shown color-coded by focal depth. Active faults are compiled from the EFSM20 database, while the principal fault segment associated with the 1904 earthquake sequence is highlighted in red. Black stars indicate the approximate epicentral areas of the 1904 earthquakes (Mw 6.9 and Mw 7.2). The distribution of contemporary seismicity delineates a pronounced WNW–ESE-oriented seismic belt spatially associated with the Krupnik fault system and adjacent fault segments. Representative focal mechanisms illustrate the dominant extensional to oblique-extensional tectonic regime in the study area. The inset map shows the location of the investigated area within the Balkan Peninsula (b).

*Corresponding Author: Emil Oynakov

Methods

The tomographic models analyzed in this study were obtained from previously published local earthquake travel-time tomography for the broader Kresna–Krupnik region. Three-dimensional distributions of P-wave velocity (Vp), S-wave velocity (Vs), and their ratio (Vp/Vs) were derived using a damped least-squares inversion scheme with smoothing constraints applied to local earthquake arrival-time data.

The inversion parameters were selected to balance model stability and data fit through damping and smoothing regularization. The inversion dataset includes both P-wave and S-wave arrival times from local and regional earthquakes recorded by the seismic network. Events with fewer than 10 arrivals and arrivals with large residuals were excluded during preliminary relocation in order to improve model robustness.

The tomographic model is based on approximately 1700 local and regional earthquakes recorded by 64 seismic stations distributed across the broader Balkan region. The dataset includes approximately 47,500 travel-time arrivals, consisting of about 32,900 P-wave and 14,600 S-wave picks.

Vp/Vs ratios were interpreted jointly with ΔVp and ΔVs in order to reduce interpretational non-uniqueness. Because elevated Vp/Vs values may result from multiple physical factors, including lithology, fluids, temperature, anisotropy, and inversion trade-offs, interpretations are based primarily on consistent spatial relationships among tomography, seismicity, active faults, and gravity observations rather than on isolated anomaly amplitudes alone.

Depth slices were extracted at fixed levels of 5, 10, 15, 20, 25, and 30 km. Composite maps representing the 20–30 km interval were constructed in order to emphasize persistent anomaly patterns observed across adjacent middle-crustal depth levels.

A vertical cross-section (A–A′) was constructed approximately parallel to the dominant orientation of the Simitli–Krupnik fault zone and the associated seismic corridor. Earthquake hypocenters located within a 12 km wide projection line were associated onto the section in order to illustrate the depth distribution of seismicity relative to the tomographic anomalies.

Frequency–magnitude distributions were evaluated primarily as supplementary indicators of catalog consistency. Because the earthquake catalog spans several decades with evolving network configuration and detection capability, these analyses are not used as primary evidence for tectonic interpretation.

Ray coverage and S-wave resolution decrease with depth. Tomography anomalies below approximately 20 km are less well constrained than shallow structures and are therefore interpreted cautiously. Detailed checkerboard and recovery tests for the original inversion are presented in Oynakov et al. (2022) and are not repeated here because the present study focuses on integrated seismotectonic interpretation rather than on inversion development.

Results

At depths of 10–15 km, both Vp and Vs anomalies are predominantly neutral to moderately positive, while Vp/Vs values exhibit pronounced lateral contrasts across the Simitli–Krupnik fault zone (Fig. 2). The fault is expressed primarily as a boundary separating crustal domains with different seismic properties rather than as a narrow localized low-velocity structure. Instrumental seismicity is concentrated preferentially along zones of strong lateral velocity gradients.

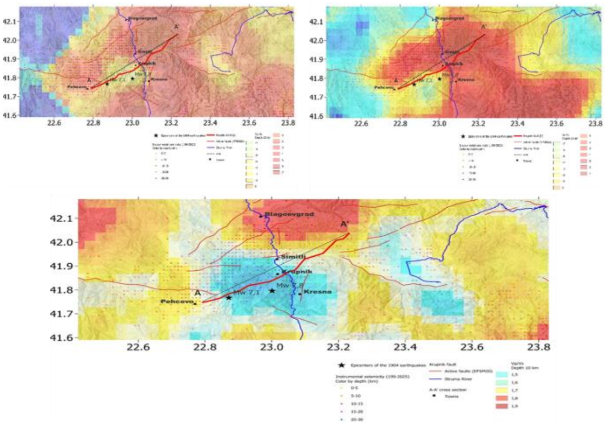

Fig. 2. Tomographic anomalies at 10 km depth: (a) ΔVp, (b) ΔVs, and (c) Vp/Vs ratio. Active faults are shown after EFSM20, while earthquake epicenters are projected from the 1991–2025 instrumental catalog. The A–A′ profile used for the vertical cross-section in Fig. 4 is indicated in panel (c). The tomography reveals pronounced lateral contrasts across the Simitli–Krupnik fault zone, with seismicity preferentially localized along velocity gradients rather than within isolated anomaly extrema.

In contrast, the 20–30 km depth interval is characterized by systematically reduced Vs anomalies (approximately –3 to –7%), while Vp anomalies remain comparatively weak or close to zero (Fig. 3). As a result, elevated Vp/Vs values locally approaching ~1.8–2.0 are observed within portions of the model. Because S-wave resolution decreases with depth, the deeper anomalies are less well constrained than shallow structures; however, the persistence of reduced Vs patterns across several adjacent depth slices suggests that the observed anomalies are unlikely to represent isolated inversion artifacts.

*Corresponding Author: Emil Oynakov

The principal tomographic characteristics and first-order interpretations for the investigated depth intervals are summarized in Table 1

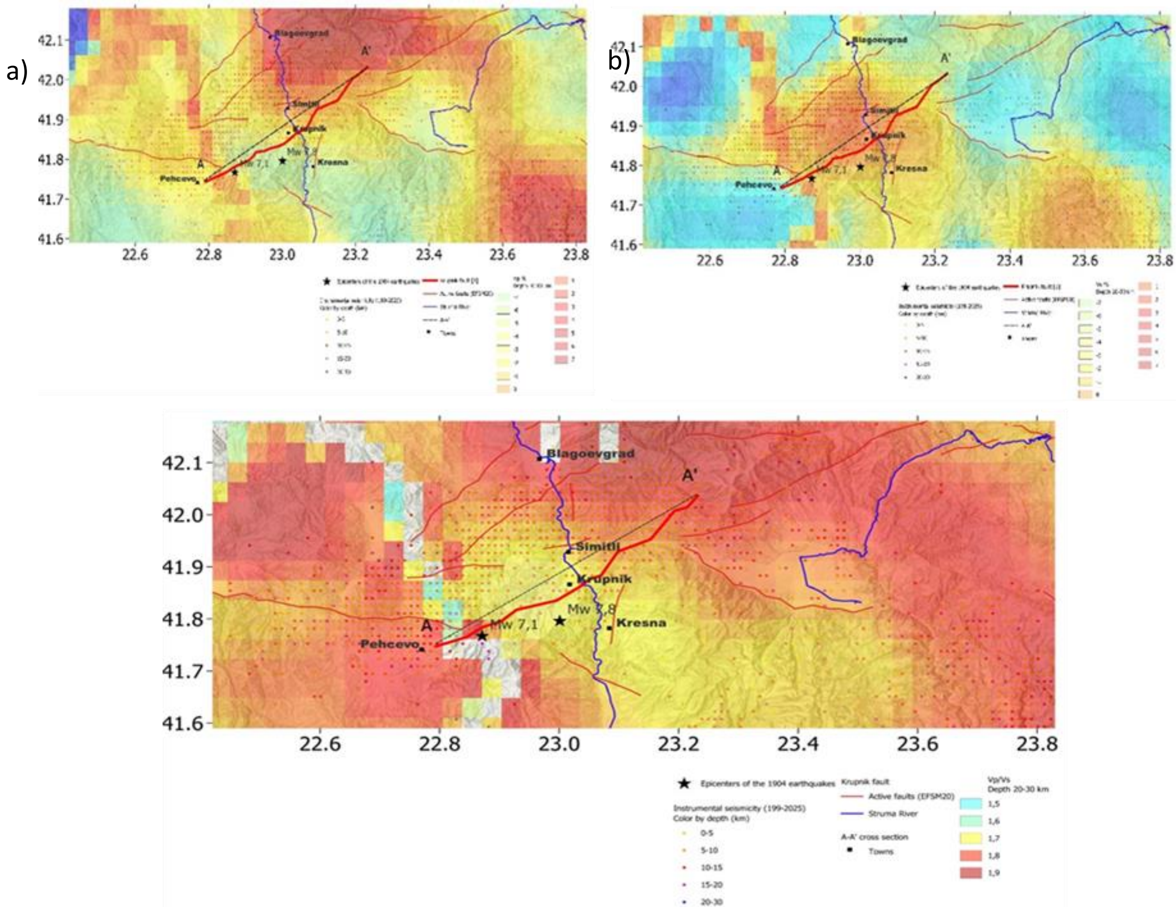

Fig. 3. Composite tomographic anomalies for the 20–30 km depth interval: (a) ΔVp, (b) ΔVs, and (c) Vp/Vs ratio. The displayed anomalies represent spatially consistent features identified by visual comparison of adjacent depth slices rather than mathematically averaged values. The maps summarize persistent anomaly patterns observed across the 20, 25, and 30 km depth slices. Earthquake epicenters from the 1991–2025 instrumental catalog and active faults after EFSM20 are superimposed. Reduced Vs values and elevated Vp/Vs ratios are observed in parts of the middle crust beneath the Simitli–Krupnik fault zone.

Instrumental seismicity is observed throughout the investigated depth interval, although the majority of earthquakes are concentrated above approximately 20 km depth. Earthquake hypocenters exhibit clear structural control and are preferentially aligned with active fault segments and lateral velocity gradients rather than with isolated velocity extrema. This spatial relationship is consistent with observations from other tectonic environments where seismicity localizes preferentially along mechanical and rheological boundaries within the crust (Ben-Zion Y. and Sammis, C.G., 2003; Eberhart-Phillips et al., 2013).

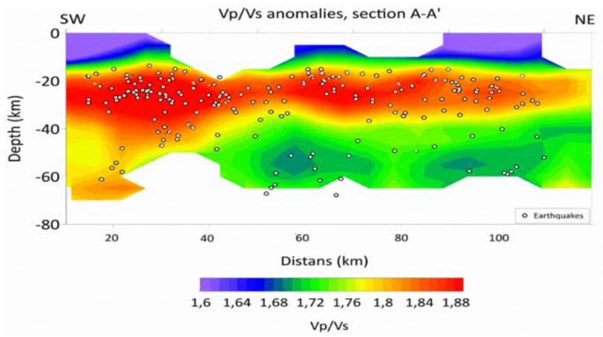

Fig. 4. Vertical cross-section along profile A–A′ approximately parallel to the dominant orientation of the Simitli–Krupnik fault zone. The upper panel shows the map position of the profile and projected earthquakes within a 12 km wide corridor. The lower panels display ΔVs anomalies and Vp/Vs values together with projected hypocenters. Earthquake symbols are shown in white with black outlines to improve visibility. Most seismicity is concentrated within the upper and middle crust, while a smaller number of deeper events extend into zones characterized by reduced Vs and elevated Vp/Vs values.

A supplementary comparison of frequency–magnitude distributions (FMD) was performed for the periods 1991–2010 and 2011–2025 in order to evaluate catalog consistency (Fig. 5). Both periods exhibit broadly comparable b-values

*Corresponding Author: Emil Oynakov

and magnitude-of-completeness estimates. Because the catalog spans several decades with evolving network configuration and detection capability, the FMD analysis is used here only as a supplementary quality-control indicator rather than as primary evidence for tectonic interpretation.

The combined tomographic, seismic, and gravity observations indicate pronounced depth-dependent structural heterogeneity within the investigated fault zone, forming the basis for the seismotectonic interpretation discussed below.

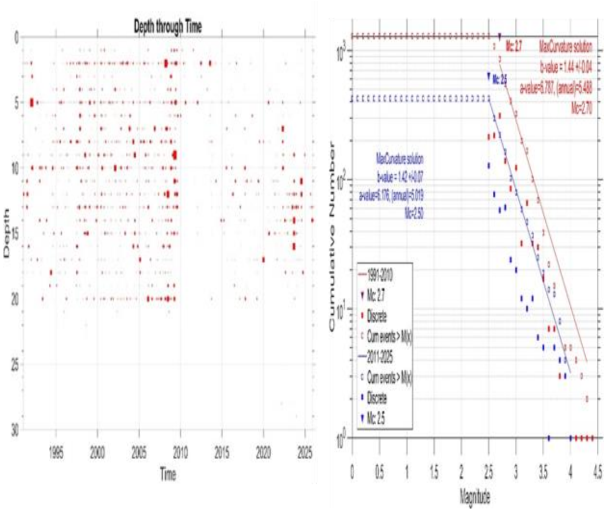

Fig. 5. Depth distribution of earthquakes during the period under consideration (a); frequency–magnitude distributions (FMD) for the periods 1991–2010 (red) and 2011–2025 (blue). Both periods exhibit similar b-values and comparable magnitude-of-completeness levels, indicating stable statistical properties of seismicity despite differences in the total number of recorded events (b).

Discussion

The combined tomographic, seismicity, structural, and gravity observations suggest a depth-dependent organization of the crust beneath the Simitli–Krupnik fault zone. At depths of 10–15 km, the predominantly neutral to moderately positive Vp and Vs anomalies, together with pronounced lateral contrasts in Vp/Vs, indicate that the fault zone is expressed mainly as a boundary between crustal domains with different seismic properties rather than as a narrow localized low-velocity structure (Fig. 2). This pattern is consistent with a comparatively coherent upper–middle crust, although this interpretation remains based on the spatial relationship between velocity anomalies, fault geometry, and seismicity rather than on direct mechanical measurements.

This depth interval is also broadly compatible with previous macroseismic estimates for the 1904 earthquakes, which suggest focal depths of approximately 15–18 km, although these values remain uncertain due to the absence of instrumental recordings. Therefore, the relationship between the 10–15 km tomographic pattern and the 1904 earthquake sequence should be regarded as interpretative rather than directly demonstrated. The coincidence between historical seismicity, present-day fault-aligned seismicity, and lateral velocity contrasts nevertheless supports the view that this part of the crust represents an important seismogenic level within the Krupnik fault system.

At depths of 20–30 km, reduced Vs anomalies and locally elevated Vp/Vs values are observed in parts of the model (Fig. 3). Such combinations may indicate a reduction in shear rigidity, but their interpretation is not unique. Elevated Vp/Vs and reduced Vs may result from several factors, including lithological variations, temperature effects, fluid presence, anisotropy, crack density, or inversion trade-offs (Christensen, N. I., 1996; Takei, Y., 2002; Karato, S. I., 2008). In addition, the tomographic resolution of S-wave velocities decreases with depth. For this reason, the 20–30 km anomalies are interpreted cautiously as possible indicators of middle-crustal heterogeneity rather than as definitive evidence for a weakened or quasi-ductile crust.

The vertical cross-section along profile A–A′ provides an additional constraint on the relationship between seismicity and the tomographic structure (Fig. 4). Most earthquakes are concentrated in the upper and middle crust, whereas only a smaller number of events extend below ~20 km. Consequently, the deeper seismicity should not be overinterpreted. Nevertheless, the projected hypocenters show a spatial association with lateral velocity gradients and with zones where reduced Vs and elevated Vp/Vs are observed. This supports the interpretation that seismicity is influenced by structural and rheological contrasts, although the limited number and uncertainty of deeper hypocenters prevent a definitive conclusion.

The Bouguer gravity anomaly provides independent but qualitative support for crustal segmentation in the study area (Fig. 6). The observed gravity gradient spatially follows the main fault zone and may reflect lateral density contrasts associated with basement structure, lithological differences, variable sedimentary thickness, or juxtaposition of crustal blocks across the normal fault system. Because gravity anomalies represent an integrated signal over depth, they cannot independently determine the depth or geometry of the causative density bodies. Therefore, the gravity data are used here as qualitative support for the structural interpretation inferred from the tomographic and seismicity patterns, rather than as an independent proof of a deep-penetrating fault.

Previous gravimetric studies in the Krupnik region (e.g., Mihailov, E. and Dimitrov, D., 2006; Dimitrov, D., et al., 2010) interpreted the observed Bouguer gradients primarily as evidence for deep-seated structural segmentation associated with the active fault system. However, gravity anomalies alone cannot uniquely distinguish between tectonic boundaries, lithological contrasts, sediment-thickness variations, or inherited basement structures. Consequently, the gravimetric interpretation should be regarded as complementary rather than definitive when evaluating the depth geometry of the fault zone.

*Corresponding Author: Emil Oynakov

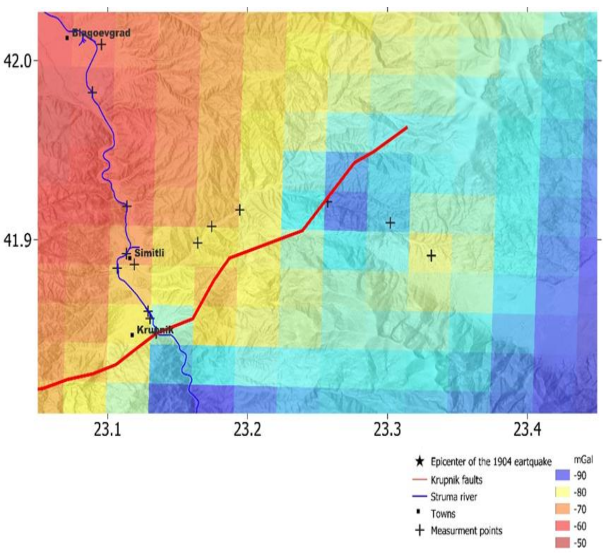

Fig. 6. Bouguer gravity anomaly map (ρ = 2.67 g/cm³) for the Krupnik region. The main fault trace (thick red line) coincides with a pronounced gravity gradient, indicating a deep-seated boundary between crustal domains with contrasting densities. The gravity pattern provides qualitative support for crustal segmentation and lateral density contrasts spatially associated with the Krupnik fault zone.

A key observation of this study is that contemporary seismicity is preferentially associated with fault segments and lateral velocity gradients rather than with isolated velocity extrema. This relationship is visible in map view and in the vertical section, where hypocenters tend to occur near zones of changing seismic properties rather than within homogeneous high- or low-velocity domains (Figs. 2–4). Similar relationships between earthquake occurrence and mechanical or rheological contrasts have been reported in other tectonic settings, where velocity gradients and fault-zone heterogeneity influence the localization of brittle deformation (Ben-Zion Y. and Sammis, C. G., 2003; Eberhart-Phillips et al., 2013).

Figure 1b shows significant distribution of depth epicenters. The edges of the faults generated recent relatively shallow seismic events outlining the seismogenic layer of shallow depth (0-10 km. with NE-SW elongated orientation). Then the change of the structure is reflected by the almost isometric second seismogenic deep layer 20-30 km. This confirms the previously indicated unilateral fault plane dipping to the NW. The asymmetry of the normal fault located and conforming the main faulting dominated structures could be easily explained as asymmetry graben effect of the 1904 earthquakes source. The visible surface faults (reaching assessed maximum amplitude of about 12 meters) are elongated in NE-SW direction. The fault plain dip is about 70^0-80^0. This explains the typical projection of surface faulting observed during the 1904 events and confirming the extensional dragging effect of the movement of Aegean sub plate rotating SW to the Kropnuk crustal block.

The integrated interpretation is also consistent with independent geodetic observations that document block-type deformation and active horizontal motions in the Struma River valley (Dimitrov, D. et al., 2010; Dimitrov, D., et al., 2019). Taken together, the tomography, seismicity, gravity, and geodetic evidence support a model in which the Simitli–Krupnik fault system acts as a structurally controlled boundary that may extend into the middle crust. However, the available data do not allow the precise geometry of this boundary at depth to be uniquely resolved.

Overall, the results support a model of a segmented, fault-controlled crust in which deformation is spatially concentrated along major structural boundaries and rheological contrasts. The interpretation emphasizes spatial consistency among independent datasets rather than relying on isolated tomographic anomalies alone. Although the deeper part of the model remains less well constrained, the observed relationships between velocity gradients, fault geometry, seismicity, and gravity anomalies provide a coherent framework for understanding the depth-dependent seismotectonic behavior of the Krupnik fault zone.

Limitations and future work

Several limitations should be considered when interpreting the results presented in this study. First, the tomographic models analyzed here are derived from previously published local earthquake tomography and therefore inherit the resolution limits and inversion assumptions of the original models. In particular, the resolution of S-wave velocities decreases with depth, and anomalies below approximately 20 km are less well constrained than shallow crustal structures. Consequently, interpretations involving the 20–30 km depth interval should be regarded as tentative and dependent on the available ray coverage and inversion stability.

Second, Vp/Vs anomalies are inherently non-unique and may reflect combinations of lithology, temperature, crack density, anisotropy, pore-fluid distribution, or inversion trade-offs. Without additional independent geophysical constraints, such as magnetotelluric, thermal, or petrophysical data, the physical origin of individual anomalies cannot be uniquely resolved. For this reason, the present interpretation emphasizes spatial relationships among tomography, seismicity, fault geometry, and gravity observations rather than relying on isolated anomaly amplitudes alone.

Third, the earthquake catalog used in this study consists primarily of routine hypocentral solutions from the Bulgarian seismic network. Although the catalog provides stable long-term instrumental coverage for the region after 1991, focal-depth uncertainty increases with depth and varies with station geometry and temporal changes in network configuration. As a result, the spatial distribution of seismicity is considered more robust than precise interpretations of individual hypocentral depths, particularly below ~20 km.

The interpretation of the Bouguer gravity anomaly also remains non-unique. Gravity data represent an integrated response to density variations over depth and cannot independently constrain the geometry or depth extent of the inferred crustal structures. Accordingly, the gravity observations are used here only as qualitative support for

*Corresponding Author: Emil Oynakov

crustal segmentation inferred from the tomographic and seismic observations.

Another important limitation concerns the relationship between the contemporary seismicity and the 1904 earthquake sequence. Although historical macroseismic estimates suggest focal depths broadly compatible with the seismogenic depth interval identified in this study, the historical earthquake parameters remain uncertain because no instrumental recordings are available. Therefore, any connection between the tomography and the 1904 rupture process should be regarded as interpretative rather than directly demonstrated.

Future work should include dedicated checkerboard and resolution tests focused specifically on the 20–30 km depth interval, relocation of the instrumental seismicity using updated velocity models, and integration with GNSS-derived deformation fields. Additional constraints from magnetotelluric, thermal, and petrophysical studies would be particularly valuable for evaluating the physical origin of the observed Vp/Vs and Vs anomalies in the middle crust beneath the Simitli–Krupnik fault zone.

Table 1. Summary of tomographic characteristics by depth intervals.

Depth interval (km)	**ΔVp (%)**	**ΔVs (%)**	**Vp/Vs**	**Seismic behaviour (1991–2025)**	**Interpretation (first-order)**
5–10	±7% (often small to moderate); local highs near fault	±7% (often small to moderate); generally similar to Vp	≈1.55–1.70 (mean ~1.60)	Shallow, densely clustered seismicity near main fault trace	Block contrast across fault; comparatively coherent shallow crust; Vp/Vs reflects composition/rigidity more than fluids
10–15	Often neutral to positive; local + anomalies near Krupnik fault	Often neutral to positive; not systematically reduced along fault	≈1.60–1.80 (local highs)	Structurally controlled seismicity aligned with fault segments	Structurally defined seismogenic boundary; sharp lateral gradients mark domain boundary; broadly compatible with inferred depths of historical earthquakes
15–20	Moderate anomalies; locally positive	Moderate anomalies; locally positive	≈1.65–1.85 (transition upward)	Distributed deep fault-controlled seismicity	Possible transitional crustal regime; increased effective Poisson's ratio
20-30	≈ –1 to +2%	–3 to –7%	≈ 1.75–2.0	Limited deeper seismicity locally associated with velocity gradients	Possible middle-crustal heterogeneity with reduced shear rigidity; reduced shear modulus; domain boundary

Interpretations presented in Table 1 are qualitative and should be considered together with the limitations discussed in the text.

Conclusions

The integrated analysis of local earthquake tomography, instrumental seismicity, active fault geometry, and gravity observations reveals pronounced depth-dependent structural heterogeneity within the Simitli–Krupnik fault zone in southwestern Bulgaria.

At depths of approximately 10–15 km, the tomographic models show predominantly neutral-to-positive Vp and Vs anomalies together with strong lateral contrasts in Vp/Vs. In this depth interval, the fault system is expressed primarily as a structural boundary separating crustal domains with different seismic properties rather than as a localized low-velocity zone. The concentration of seismicity along lateral velocity gradients suggests that deformation is preferentially localized along rheological and structural contrasts within the crust.

At depths of approximately 20–30 km, reduced Vs anomalies and locally elevated Vp/Vs values are observed in parts of the model. Because these anomalies are less well constrained than shallow structures and because Vp/Vs variations are inherently non-unique, they are interpreted cautiously as possible indicators of middle-crustal heterogeneity and reduced shear rigidity.

The combined tomographic, seismic, and gravity observations support the interpretation of the Simitli–Krupnik fault zone as a structurally controlled crustal boundary that may extend into the middle crust. Contemporary seismicity exhibits strong spatial association with fault segments and velocity gradients rather than with isolated anomaly extrema.

Although the deeper crustal structure remains insufficiently constrained, the observed consistency among independent

*Corresponding Author: Emil Oynakov

datasets provides a coherent framework for understanding the depth-dependent seismotectonic behavior of the Krupnik fault system and its role within the actively deforming Struma River valley region.

The geodynamics of the investigated area falls in the predominant extensional regime. The extensive registrations of great amount local seismic events (about 85-90% of all weak earthquakes registered in Bulgaria), together with the intensive displacements established by the GNSS network and the structural control of seismicity as shown in this study are conditions providing possible expectation for very strong earthquakes similar to those of 1904.

Acknowledgments

The presented work was performed within the project Assessment of Earthquake Ground Motion Amplification in the Sofia Basin, funded by the Bulgarian National Science Fund, contract number КП-06-Н64/1 from 15.12.2022.

References

1. Christoskov, L., Sokerova, D., & Rijikova, S. (1978). Catalogue of the Historical Earthquakes in Bulgaria. Funds of the Geophysical Institute, Bulgarian Acad. Sci., Sofia.
2. Ambraseys, N. N. (2001). The Kresna earthquake of 1904 in Bulgaria. Ann. Geophys., 44(1).
3. Ranguelov B, Rizhikova S, Toteva T (2001) Some data for the magnitude reevaluation of the strong earthquakes during 1904 in Kresna–Kroupnik zone (SW Bulgaria). The Earthquake (M7.8) Source Zone (Southwest Bulgaria), Professor: Drinov M Academic Publishing House, pp 266–269.
4. Meyer, B., Armijo, R., & Dimitrov, D. (2002). Active faulting in SW Bulgaria: possible surface rupture of the 1904 Struma earthquakes. *Geophysical Journal International*, *148*(2), 246-255.
5. Protopopova, Valentina and Emil Botev (2020): "Evaluation and comparative analysis of stress and deformations in seismic hazard zones in Bulgaria and adjacent lands." *Annals of Geophysics* 63, no. 2 GD224-GD224.
6. Dimitrov, D., Botev, E., & Georgiev, I. (2010). Results from monitoring of the Krupnik seismogenic area in SW Bulgaria. Geol. Balc., 39(1–2), 93.
7. Scholz, C. H. (2002). The Mechanics of Earthquakes and Faulting, 2nd ed. Cambridge Univ. Press, Cambridge.
8. Bürgmann, R., & Dresen, G. (2008). Rheology of the lower crust and upper mantle: Evidence from rock mechanics, geodesy, and field observations. Annu. Rev. Earth Planet. Sci., 36, 531–567.
9. Dimitrov, D. (2019). Regional Bouguer gravity anomaly dataset for Southwest Bulgaria (2.67 g/cm³ reduction density). National Institute of Geophysics, Geodesy and Geography, Bulgarian Academy of Sciences (Personal Communication / Digital Data Repository).
10. Oynakov, E., Aleksandrova, I., Popova, M., & Ranguelov, B. (2022). Seismic tomography model of earth crust of SW Bulgaria and surroundings. Bulg. Geophys. J., 45, 68-79.
11. Ben-Zion, Y., & Sammis, C. G. (2003). Characterization of fault zones. Pure Appl. Geophys., 160(3), 677–715. https://doi.org/10.1007/PL00012554
12. Eberhart-Phillips, D., Reyners, M., Faccenda, M., & Naliboff, J. (2013). Along-strike variation in subducting plate seismicity and mantle wedge attenuation related to fluid release beneath the North Island, New Zealand. Phys. Earth Planet. Int., 225, 12–27.
13. Christensen, N. I. (1996). Poisson’s ratio and crustal seismology. J. Geophys. Res., 101(B2), 3139–3156.
14. Takei, Y. (2002). Effect of pore geometry on VP/VS: From equilibrium geometry to crack. J. Geophys. Res., 107(B2), ECV-6.
15. Karato, S. I. (2008). Deformation of Earth Materials: An Introduction to the Rheology of the Solid Earth. Cambridge Univ. Press, Cambridge.
16. Mihailov, E., & Dimitrov, D. (2006). Results from gravimetric measurements in the region around the Krupnik fault, SW Bulgaria. Geodesy, 7, 108–115.

*Corresponding Author: Emil Oynakov